Formation of Entanglements at Brushlike Interfaces in Cellulose–Polymer Composites

JOHAN M. FELIX and PAUL GATENHOLM*

Department of Polymer Technology, Chalmers University of Technology, S-412 96 Göteborg, Sweden

SYNOPSIS

Cellulose fibers were grafted with compatibilizing agents, such as maleated polypropylenes of different molecular weights. Steric effects and surface free-energy effects were found to stimulate the stretching of grafted chains away from the cellulose fiber surface, giving rise to a brushlike configuration in a polypropylene (PP) melt. Inverse gas chromatography measurements on modified fibers using a model compound for PP as adsorbate showed that interactions of PP and grafted fibers, which were mainly diffusion-dependent, increased with increasing molecular weight of the compatibilizer. Dynamic mechanical measurements and tensile testing of composites showed that the presence of compatibilizing agents enhanced stress transfer and increased interphase thickness considerably, the most significant effect being obtained for the high molecular weight compatibilizers. Apparently, the longer the grafted chains, the larger the fraction of matrix molecules involved in the interactions and, thus, the thicker the interphase. The improvement of adhesion between treated fibers and PP, as detected by peel testing, was proven to be caused mainly by entanglements formed between compatibilizing agents and PP. © 1993 John Wiley & Sons, Inc.

INTRODUCTION

Extensive research has been carried out over the past 10 years in the field of wood cellulose-reinforced thermoplastics.[1-3] Initially, scientists faced the problem of the incompatibility of hydrophilic cellulose fibers and hydrophobic thermoplastic matrices, which yielded composites with poor properties. It has been shown, however, that the use of compatibilizing and coupling agents for treating fibers prior to, or as an addition in, the compounding step results in improved mechanical properties.[4] Graft polymers of the matrix material and a polar group, e.g., maleated polypropylene (MAPP), have been particularly successful in cellulose–polypropylene composites, because, in addition to improving tensile strength, they also increase impact strength.[5,6] These improvements are believed to be a consequence of enhanced interfacial adhesion.

The character of the interface has long been known to determine properties of multicomponent systems. In particular, interactions across interfaces have been ascribed a crucial role. Adhesion mechanisms proposed in the literature have not only stressed the effect of chemical bonds at the interface, but have also recognized the influence of the physical properties of the interfacial region or the interphase.[7,8] Among other adhesion mechanisms, authors have reported interdiffusion between neighboring polymers to be of major importance for bonding between the phases.[9-12] As a result of interdiffusion, entanglements are formed that link the components. Cho et al.[13] showed that diffusion of a polymeric adhesive into both sides of a joint is crucial for high joint strength. The interpenetration of macromolecular chains at the polymer–polymer interface at temperatures above the glass transition is treated by the diffusion theory of polymer adhesion,[14] which states that molecular bridges formed as a result of self-diffusion are responsible for adhesive strength. In the case of semicrystalline polymers, the diffusion primarily takes place in the less dense and more mobile disordered regions that separate the denser, ordered crystalline lamellas.[15]

In a previous investigation, we explained the nature of the link between the MAPP compatibilizer

* To whom correspondence should be addressed.

Journal of Applied Polymer Science, Vol. 50, 699–708 (1993)
 CCC 0021-8995/93/040699-10

and cellulose fiber by showing that MAPP is covalently bonded to the fiber surfaces through transesterification.[16] However, the character of the interactions between the MAPP attached to the cellulose surface and PP matrix has not been investigated. In this study, we, therefore, aimed to elucidate the contribution of entanglement formation to the interaction balance. MAPP chains of different lengths were grafted to a cellulose surface and the structure and dynamics of these chains are discussed partly in terms of the brush concept.[17] Dynamic mechanical thermal analysis was used for detecting immobilization of matrix molecules at the fiber/matrix interface. Interphase thickness values calculated from composite yield stress data according to Pukánszky et al.[18] are taken as a measure of the extent of immobilization or interdiffusion. A more direct, quantitative correlation between interdiffusion and practical adhesion was obtained using peel testing.

THE CONCEPT OF POLYMER BRUSHES

When a long-chain polymer is attached to a surface or an interface, the mobility of the chains is restricted. Normally, the grafted chains would adopt a random-walk configuration in order maximize their configurational entropy.[17] However, under certain conditions, the grafted chains may stretch away from the surface and form a brushlike structure. Particularly important factors that affect the stretching tendency are graft density, the molecular weight of grafted chains, and the character of the surrounding medium.[19] A high graft density, σ, allows neighboring chains to overlap. Thus, they must stretch away from the surface in order not to overfill space. The adopted conformations lead to a brush height, h, that grows faster than the typical chain dimension, R_g, when the molecular weight increases. The interactions of the grafts with the surrounding medium are also of vital importance, especially when the medium is a solvent. As brush formation is likely to occur in numerous systems, e.g., in solutions or melts containing block copolymers as surfactants or compatibilizers, great effort has been taken to understand and describe these systems in theory.[20–27] Two major approaches have been developed for analysis, namely, the scaling argument[20,21] and the self-consistent field theory.[22–24]

These theories have primarily been applied for describing brushes under good solvent conditions. The present case in which the brush is surrounded by a melt has not been as extensively analyzed and we will therefore only discuss our results qualitatively according to the principle of the brush concept. It should be noted that, in the discussion, we assume for the sake of simplicity that brushes are monodisperse, i.e., all chains in each compatibilizer are of the same molecular weight (M_w) and are attached in the same mode to the surface. Moreover, we assume a uniform distribution of grafting sites.

EXPERIMENTAL

Materials

Polypropylene (PP)

Commercially available PP (Trespaphan NNA 30, Hoechst AG, Germany) with a weight-average molecular weight of 268,000 g/mol was used in all experiments.

Compatibilizing Agents

Three different compatibilizers were used: one alkenylsuccinic anhydride and two PPs of different molecular weights, grafted with the same monomer (maleic anhydride). The alkenylsuccinic anhydride (ASA), with a molecular weight of 350 g/mol, was commercially available (Ethyl Corp., USA), as were the two PPs with molecular weights of 39,000 (Hercoprime G, Hercules Inc., USA) and 4500 (Epolene 43, Eastman Kodak Chemical, USA). Both PPs were modified to contain a 6 wt % maleic anhydride.

Cellulose Fibers

α-Cellulose (Nymölla AB, Sweden), obtained from 60% beechwood and 40% birchwood, was used for dynamic contact angle and inverse gas chromatography (IGC) measurements. It was also employed in composites subjected to tensile testing and DMTA experiments.

In addition to cellulose, the fibers consisted of 13% hemicellulose, 0.3% ash, and a negligible amount of lignin. The specific surface area, as determined by BET adsorption isotherms with krypton, was 1.77 m^2/g. Greaseproof paper, made of bleached sulfite pulp without additives, was used for peel tests. Extraction with dichloromethane using the SCAN-C 7 : 62 standard method determined the content of extractives to be 0.5%, most of which consisted of fatty acids and rosin acids.

Solutes

Toluene of analytical grade was used as received for the surface treatments of fibers. Squalane, used as a model compound for PP at the IGC measurements, was of chromatographic grade.

Methods

Fiber Treatment

Before treatment, cellulose fibers were Sohxlet-extracted with toluene for 24 h and dried at 70°C in an oven with circulating air for 24 h. The fibers were then immersed in a solution of compatibilizer in hot toluene (100°C) for 5 min. The weight ratio of compatibilizer to cellulose fiber in the solution was 5 : 100. After treatment, the fibers were Sohxlet-extracted with toluene for 48 h to remove all components not covalently bonded to the fibers. Finally, the fibers were dried as described above until constant weight was achieved.

Titrimetric Measurements

Determinations of acid, saponification, and hydroxyl values of cellulose fibers were performed according to a procedure described elsewhere.[28]

Contact Angle Measurements

The dynamic contact angle analyzer Cahn DCA-322 was used to measure advancing and receding contact angles according to the procedure described by Westerlind and Berg.[29] Individual untreated cellulose fibers, purified as described above, were isolated by evaporating water (while stirring) from dispersions of low amounts of fiber in distilled water. This was followed by careful drying. Treated fibers were made hydrophobic in the treatment step and needed no extra procedure for separation. The individual fibers, being typically 4 mm long, were mounted by pinching their ends in a folded aluminum foil of several layers thickness. This procedure is described in detail elsewhere.[30] The PP sample, in the shape of a rectangle of the dimensions 10 × 30 mm, was cut from a 60 μm-thick film and washed in isopropanol in an ultrasonic bath for 10 min. The contact liquids used were distilled water and diiodomethane, and the surface energy components were calculated by using the harmonic mean equation. Immersion rate was 20 μm/min and immersion depth was typically 2 mm. Average values from 6 to 8 measurements of each type of fiber were used for calculations. The standard deviation did not exceed 6.1% for any of the samples.

Inverse Gas Chromatography (IGC)

Typically, a 1 m-long stainless-steel column of $\frac{1}{4}$ in. o.d. was degreased, washed, and dried before packing. Between 3.71 and 4.44 g of carefully dried cellulose was packed into the column. Measurements were performed on a Varian 3400 gas chromatograph equipped with a flame-ionization detector. Helium was used as the carrier gas, and the flow rate was typically 30 mL/min, as measured frequently with a soap bubble flowmeter. Two columns of each cellulose sample were investigated and an average of at least five readings was made on every occasion. The readings usually agreed within 2%. Methane was used as an inert marker for the dead volume of the column, and correction was made for any pressure drop across the column. The probes (squalane) were injected with 1 μL Hamilton syringes, and each injection was repeated several times, showing elution peaks to be reproducible. The injection and detection temperatures were kept at least 50°C above the boiling point of the solute in question. The experiments were performed at 373 K. Retention times, peak heights, and peak areas were given by a Varian GC Work Station.

Preparation of Composite Samples

For DMTA and tensile testing, the fibers and the matrix material were mixed and homogenized in a Brabender mixer. The average residence time was in the order of 5 min and the temperature 180°C. The mixes were compression-molded at 180°C for 3 min into sheets that were quenched in liquid nitrogen. DMTA specimens of the dimensions 12 × 50 × 2 mm and dog-bone-shaped specimens for tensile testing were cut from the sheets. All samples contained 40 wt % cellulose fibers. For peel tests, samples were prepared as three-layer laminates in a hot press. A 60 μm-thick PP film was placed between two sheets of grease-proof paper, after which a pressure of 4 bar was applied for 3 min at 180°C. A 40 μm-thick frame of aluminum foil was placed between the paper sheets and ensured a uniform thickness of the PP layer obtained in the laminate.

Dynamic Mechanical Thermal Analysis (DMTA)

A DuPont 983 DMA was used for measurements, performed at a frequency of 1 Hz. The heating rate was 4°C/min (no significant difference was noted between results obtained at 2°C/min and those at 4°C/min), and the measurements stretched over the temperature range of −70 to 170°C. Three samples of each blend were analyzed. The standard deviation was less than 3.7% and did not affect the relative position of the curves.

Tensile Testing

An Instron tensile tester (Instron 1193, extensometer G51-15MA) was used for obtaining stress–strain data of the composites. The strain rate was 1.1

$\times 10^{-3}$ s^{-1} and the temperature 23 ± 0.5°C. All results are the average values of five measurements. The maximum standard deviation was 4.1%.

Adhesion (Peel) Test

To measure the practical adhesion between the layers, the laminates were tested by means of T-peel testing equipment (Minimat, Polymer Labs) at 23°C and 50% relative humidity. The peel rate was 100 mm/min. Five samples of each laminate were analyzed. The relative standard deviation did not exceed 5.5%.

RESULTS AND DISCUSSION

Surface Configuration

Alkyl chains and PP chains of various lengths were attached to cellulose fiber surfaces by chemical bonding of different compatibilizers, described in Table I, to cellulose. Bonding occurred owing to the formation of an ester linkage between succinic moieties of the compatibilizers and hydroxyl groups of the cellulose surface. Evidence of this chemical reaction was obtained by FTIR.[16]

As opposed to ASA, the MAPP compatibilizer is, considering the structure, not an exactly defined molecule with only one functional group that can provide covalent bonding to a cellulose surface. It is composed of randomly grafted PP chains with several bonding sites distributed along the chains. Thus, many different attachment modes of MAPP to cellulose theoretically exist. To gain an understanding of the attachment modes, we used titration to determine the extent of transesterification, which gives the number of bonding sites involved in the immobilization process. From gravimetric measurements on fibers before and after treatment, the amount of MAPP bonded to the cellulose and, hence, the grafting density (chains per surface area unit) was determined. However, although the average number of acid groups reacted per MAPP chain is known, their positions along the PP chain are not defined. Thus, to calculate the range of possible lengths of chain segments that can stretch away from the cellulose surface, one must consider the two extreme cases: Either all the acid groups are grafted onto the end of the PP chain, giving a tail configuration when reacted with cellulose, or they are evenly distributed along it (loop configuration). In the present paper, these cases will be designated as the maximum and minimum lengths, respectively.

Steric Effects on Stretching

Tables II and III show a summary of the extent of grafting reactions, the grafting density σ, the distance between grafting sites $\sigma^{-1/2}$, and the calculated minimum and maximum lengths of chain segments that are able to stretch away from the surface. The alkenylsuccinic anhydride is a true end-grafted molecule that, owing to its short chain length, is relatively limited (compared to polymers) in its conformational behavior. As the average distance between grafting sites is 0.46 nm, as compared with the linear chain dimension of about 2.6 nm, an orientation of the chains perpendicular to the surface is most probable in order to avoid overlapping. Thus, when an ASA-treated fiber is introduced into a reasonably good solvent, the alkyl chains will stretch and form a brush with a height close to 2.6 nm. An evaluation of the results obtained for the maleated PPs is more complicated. For the medium-length compatibilizer (B), free chain segment lengths reach at maximum about 97 propylene units (tails) and at minimum 49 units (loops). Assuming that MAPP has an isotactic helix structure—which should be correct, as a minimum of 5 units are required to maintain a helical conformation[31]—the maximum brush height can be estimated (see Table III). Comparing the calculated lengths for the two configurations with the graft density, we find that the graft density seems high enough to favor stretching in both cases. The free segments are longer for the compatibilizing agent of the highest molecular weight (C), but at the same time, the graft density is lower. However, the ratio of graft site distance to

Table I Compatibilizing Agents Used for Surface Treatment of Cellulose

Compatibilizer	MW of Compatibilizer (g/mol)	Chemical Structure of Compatibilizer
A (ASA)	350	Alkenylsuccinic anhydride
B (Epolene 43)	4,500	Polypropylene grafted with 6% maleic anhydride
C (Hercoprime)	39,000	Polypropylene grafted with 6% maleic anhydride

Table II Extent of Transesterification of Cellulose, Graft Density, and Graft Distance of Compatibilizer on the Surface

Type of Fiber	Average No. COOH Groups per Molecule	Average No. Reacted with Cellulose	Graft Density, σ (grafts/nm^2)	Graft Distance, $\sigma^{-1/2}$ (nm)
Treated (A)	2.0	1.5	4.8	0.5
Treated (B)	5.4	3.2	1.5	0.8
Treated (C)	47.3	13.7	0.2	2.2

free segment length suggests that stretching is still likely to occur owing to the dense population of relatively long grafts on the surface.

Surface Free-energy Effects

The surface energy data obtained by dynamic contact angle analysis are presented in Table IV. The polar or the nondispersive component of the surface energy of pure cellulose was dramatically decreased by all treatments, whereas the dispersive energy increased slightly. This was a further indication of the efficiency of the treatments.

Interfacial tension between fiber surface and matrix is a factor that influences the structure and character of the interphase. For components that do not interpenetrate at the interface, the interfacial tension, γ_{12}, is calculated according to the harmonic mean equation, which is valid between low-energy materials[32,33]:

$$\gamma_{12} = \gamma_1 + \gamma_2 - \frac{4\gamma_1^d\gamma_2^d}{\gamma_1^d + \gamma_2^d} - \frac{4\gamma_1^p\gamma_2^p}{\gamma_1^p + \gamma_2^p} \quad (1)$$

where γ_1 and γ_2 are the surface tensions of solid 1 and 2, respectively, and d and p denote the dispersive and polar (nondispersive) component, respectively.

In the present case, this expression can be applied correctly only on the untreated fiber/PP system, in which the interactions are exclusively surface-dependent. When the compatibilizing agent is present on the fiber surface, interpenetration, which is not taken into consideration in eq. (1), may affect interfacial energetics. However, the surface tensions of the interpenetrable phases can be discussed qualitatively when estimating the willingness of these phases to wet and diffuse into each other. For the untreated fiber/PP system, the γ_{12} value of 41.0 mJ/m^2 obtained indicates total incompatibility between fiber and matrix. Comparing surface tension of the PP matrix with that of the treated fibers, it is suggested that these systems are more compatible.

These observations have some important consequences for the conformational behavior of compatibilizer chains: As the hydrocarbon blocks in the compatibilizers exhibit a high interfacial tension versus the cellulose, this tension can be expected to stimulate stretching of grafted chains. Moreover, as the compatibilizer phases possess surface energy profiles and solubility parameters similar to those of the matrix, the grafted chains should mix with the matrix, a fact favoring stretching.

Estimation of Interfacial Interactions

Interactions between the different cellulose surfaces and the PP matrix were studied with IGC using a squalane molecule as a structured model compound for a PP macromolecule (see Fig. 1). IGC measurements provide a specific retention volume, which, at temperatures above the glass transition of the stationary phase, is chiefly a measure of the solubility of the probe molecules (squalane) in the stationary phase (compatibilizing agent and cellulose).

Table III Lengths of Chain Segments that Can Stretch Away from the Cellulose Surface (Isotactic Helix Structure of MAPP Chains Is Assumed)

Type of Fiber	Minimum Free Length	Maximum Free Length	Theoretical Brush Height of Fully Stretched Compatibilizer Chains (Minimum – Maximum) (nm)
Treated (A)	20 carbon atoms	20 carbon atoms	2.6
Treated (B)	49 propylene units	97 propylene units	11–21
Treated (C)	74 propylene units	867 propylene units	16–188

Table IV Surface Energies of Fibers and Matrix

Sample	Surface Free Energy (mJ/m^2)	Nondispersive Component (mJ/m^2)	Dispersive Component (mJ/m^2)
Untreated fiber	68.7 ± 3.9	43.2 ± 2.7	25.5 ± 1.2
Treated (A)	49.8 ± 4.5	21.8 ± 2.3	28.0 ± 2.2
Treated (B)	40.0 ± 2.6	8.4 ± 1.0	31.6 ± 1.6
Treated (C)	36.9 ± 2.8	4.9 ± 1.1	32.0 ± 1.7
Polypropylene	32.7 ± 1.3	1.0 ± 0.4	31.7 ± 0.9

Thus, the specific retention volume could serve as an indication of the intermolecular interactions, principally in the form of interdiffusion between compatibilizer and matrix chains. Figure 2 shows the effect of molecular weight of the compatibilizer used for surface treatment on the specific retention volume of squalane. Retention volumes were normalized to the weight load of compatibilizer on the fibers. It was found that the specific retention volume increased with an increasing molecular weight of the compatibilizer. This result suggests that the longer the grafts the more extensive the diffusion process.

Adhesion and Interphase Thickness

In the discussion of interfacial adhesion, we will only treat interactions in the amorphous phase. To minimize the influence of interactions in crystalline regions of the interphase, all samples used were quenched from the molten state with liquid nitrogen. In this way, PP composites with a relatively low degree of crystallinity (~ 30%, from DSC) were obtained.

Stretching of grafts and interdiffusion in the composite melt are phenomena likely to affect the degree of interfacial interactions and, accordingly, the interphase structure. To investigate this effect, dynamic mechanical measurements, tensile testing, and peel testing were employed.

Results of dynamic mechanical measurements on cellulose–PP composites are shown in Figure 3 where tan δ is plotted as a function of temperature. The introduction of untreated cellulose fibers into the PP matrix causes a slight broadening of the tan δ (α-) peak at around 5°C, characteristic of the glass transition, but not a significant upward shift of the peak. Adding treated fibers changes the curve considerably, proving strong interactions. Tan δ is significantly reduced and the α-peak is shifted between 2 and 5°C upward. This effect is most pronounced for the sample composed of PP and fibers treated with the compatibilizer of the highest molecular weight.

Interfacial characteristics have frequently been derived from tensile properties of composites. The yield stress, σ_y, has been regarded as a particularly important parameter, as it provides information on the maximum allowable stress that will not cause considerable plastic deformation. However, the yield stress is also influenced significantly by microstructural features such as filler/fiber shape, its size and dispersion, and interphase volume. This has complicated the development of theoretical relations between yield stress and composition. A semiempirical interpretation route that has been applied on heterogeneous polymer systems, such as $CaCO_3$-reinforced PP, was developed by Pukánszky and coworkers.[18,34-37] According to this concept, the yield stress of a composite is expressed as

$$\sigma_y = \sigma_{y0} \frac{1 - \varphi_f}{1 + 2.5\varphi_f} \exp(B\varphi_f) \qquad (2)$$

where σ_y and σ_{y0} are the composite and matrix yield stresses, respectively; φ_f, the volume fraction of the filler; and B, is a parameter characterizing stress transfer to the dispersed phase. Thus, yield stress

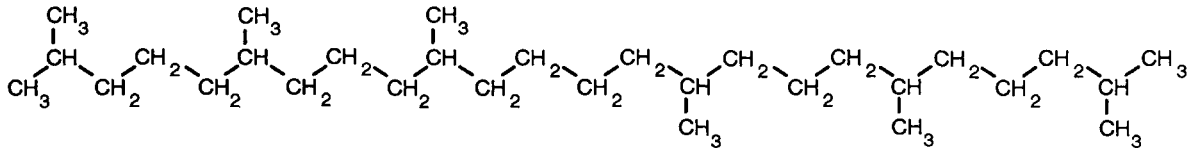

Figure 1 Chemical structure of squalane that was used as model compound for PP.

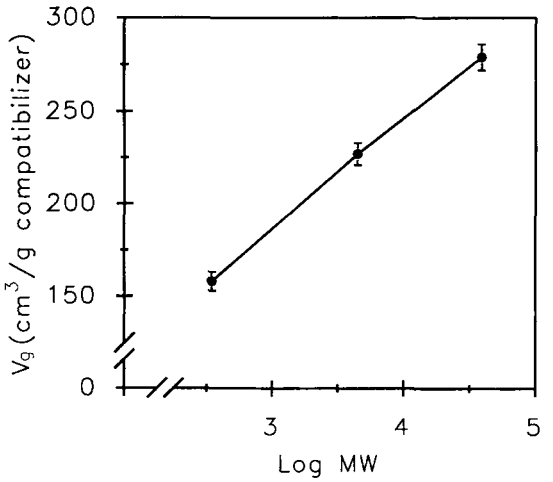

Figure 2 The effect of the molecular weight of the grafts on the retention volume of squalane. Mean values and errors are obtained from the analysis of two columns of each sample (at least five injections were made in each column).

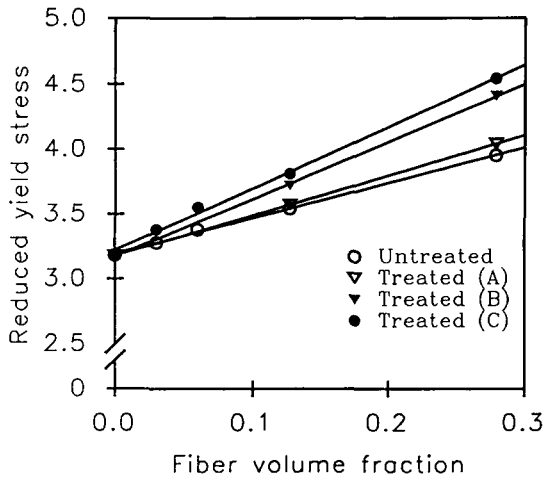

Figure 4 Semilogarithmic plot of the reduced yield stress ($\sigma_y[1 + 2.5\varphi_f]/[1 - \varphi_f]$) for the composites as a function of composition. The stress transfer parameter B was calculated from the slopes.

of the composite is determined mainly by three factors: the yield stress of the matrix, the interfacial interactions $\exp(B\varphi_f)$, and the decrease in effective load bearing cross section of the matrix as an effect of filling: $(1 - \varphi_f)/(1 + 2.5\varphi_f)$. It follows from eq. (2) that weak interactions, i.e., $B \approx 0$, cause a continuous decrease in σ_y with increasing filler content.

Parameter B is dependent on a large number of factors, among which we find the reinforcing effect of filler (shape and aspect ratio), homogeneity of composite (filler dispersion), stress distribution, and concentration and interactions (filler–matrix, filler–filler). For a system containing a spherical filler, B can be expressed as

$$B = (1 + I\rho_f A_f) \ln \frac{\sigma_{yi}}{\sigma_{y0}} \qquad (3)$$

where A_f and ρ_f are the specific surface area and density, respectively, of the filler, and σ_{yi} and I are the yield stress and the thickness, respectively, of the interphase. When using this expression for a fiber-containing system, it should be noted that the expression does not take into consideration the fiber orientation factor or the reinforcing effect of a fiber

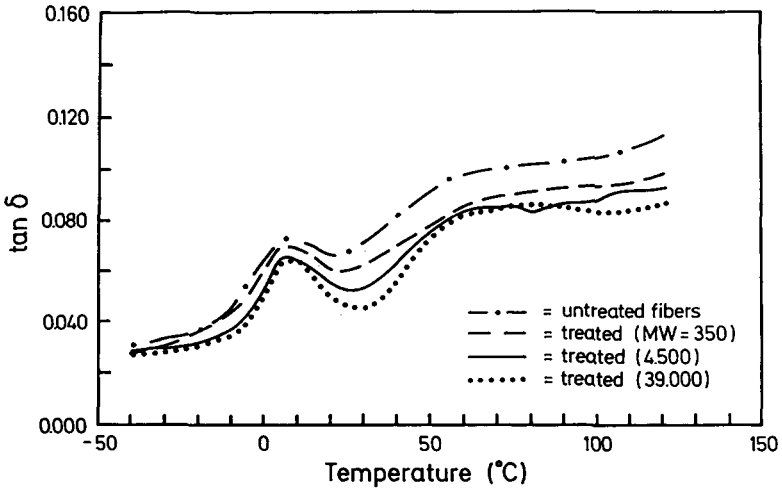

Figure 3 Dynamic mechanical spectrum of cellulose fiber/PP composites. Tan δ as a function of temperature.

Table V *B* Values for the Composites as Calculated from the Slopes of the Plots in Figure 4

Type of Fiber	*B*	Accuracy of Fit, r^2
Untreated	2.77	0.995
Treated (A)	3.08	0.997
Treated (B)	4.43	0.998
Treated (C)	4.87	0.995

owing to its geometry. However, as the orientation factor should be about the same in all samples and as the treatments used do not influence the fiber aspect ratio obtained after the compounding step, the same relative error is inflicted on all interphase thickness values. A more detailed theoretical treatment of the yield stress results obtained in this study is presented elsewhere.[38]

To verify the validity of the theory for the present composites, the reduced yield stress ($\sigma_y[1 + 2.5\varphi_f]/[1 - \varphi_f]$) was plotted as a function of composition in a semilogarithmic plot. As shown in Figure 4, straight lines were obtained, suggesting that

- Equation (2) is indeed valid for the system;
- The composites are homogeneous;
- The treatments have strong and nonlinear effects on properties; and
- The compatibilizers do not change matrix properties, i.e., intercept value corresponds to the matrix value.

B values, which were calculated as the slope of the straight lines, are presented in Table V. Stress-transfer efficiency is enhanced considerably by treatments, increasing with the molecular weight of compatibilizing agent.

In eq. (3), which was applied for a rough calculation of the interphase thickness, there are two unknown factors, *I* and σ_{yi}. Pukánszky et al. calculated the latter parameter by assuming that only secondary forces were involved in the interactions creating the interphase.[18] A linear relationship between the reversible work of adhesion and the interphase thickness was found in filled PP, which we applied in this study. As the work of adhesion for the different cellulose/PP composites differed little, the interphase yield stresses obtained were similar (see Table VI). This procedure for obtaining σ_{yi} yields only approximative values, particularly because it neglects the influence of interdiffusion on interphase yield stress. The importance of interdiffusion is indicated by the fact that although the work of adhesion does not vary considerably for different treatments the *B* value does. However, in the case of ASA-treated or untreated fibers, where interdiffusion cannot be a significant interaction mechanism, the procedure is useful. Inserting σ_{yi} data into eq. (3), interphase thickness values were obtained that increased with the molecular weight of compatibilizer. Although σ_{yi} values for the high molecular weight compatibilizers are approximative, it should be noted that even if deviations as high as 50% were inflicted on these σ_{yi} values, i.e., the real values were about 50% larger than given in the table, the trend would still be the same. This fact confirms that the MAPP chains do stretch away from the cellulose surface, interfering with more matrix molecules and thus increasing the volume of the interphase. The enhancement of mechanical properties is then plausible owing to entanglements formed at the interface.

The values of interphase thickness seem unreasonably high. However, it should be stressed that these values are by no means absolute. First, they are indirectly calculated from results of mechanical tests and, second, they suffer from the fact that simplifying assumptions are made in the calculations. Moreover, we must bear in mind that the use of a property-oriented technique yields a "dynamic thickness" of the interphase, being much larger than

Table VI Interphase Thicknesses Calculated According to Eq. (3); Parameters Used for the Calculations Are Also Listed

Type of Fiber	A_f (m^2/g)[a]	ρ_f (g/cm^3)	σ_{y0} (MPa)	σ_{yi} (MPa)	*B*	*I* (μm)
Untreated	1.77	1.57	24.0	45.8	2.77	1.19
Treated (A)	1.74	1.57	24.0	45.5	3.08	1.40
Treated (B)	1.30	1.57	24.0	45.6	4.43	2.89
Treated (C)	1.11	1.57	24.0	45.3	4.87	3.83

[a] From Ref. 39.

the static values obtained from structure-probing techniques or theoretical calculations/models.[40]

A technique generally used for adhesion measurements is peel testing of laminates.[41,42] This method has been used extensively for evaluating the influence of interdiffusion on adhesion.[9,43] In the present systems, we know that surface properties (energetics, acid–base character, etc.) of treated cellulose samples are rather similar.[44] Thus, when comparing the peel strengths of these samples with PP, we consider any difference as primarily being a result of variations in the work required for disentanglement. For interpreting data in this manner, it was necessary to be assured of interfacial failure in the laminates, a condition that was checked by ESCA analysis of the cellulose and PP surfaces before compounding and after peel testing. No significant differences in the O/C ratios were detected between these measurements, hence, indicating interfacial failure.

Results of peel tests are presented in Figure 5. Taking the standard deviation into consideration, peel strength is increased by, at least, 55% as a consequence of the surface treatment that introduces short grafts. With an increasing MW of the compatibilizer (treatment with B and C), the peel strength increases by a factor 1.3–1.6 further (as compared to treatment with A). Interdiffusion of chains at the interface is apparently a phenomenon of great significance in the interaction balance. If stretching of graft chains may occur, a thicker interphase is created owing to a more extensive immobilization of matrix chains through formation of entanglements. The MAPP grafts (B and C) seem to possess sufficient molecular weights and internal

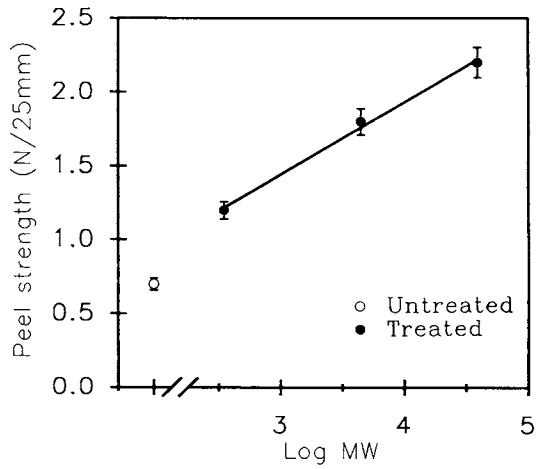

Figure 5 The effect of molecular weight of compatibilizer on peel strength of cellulose/PP laminates.

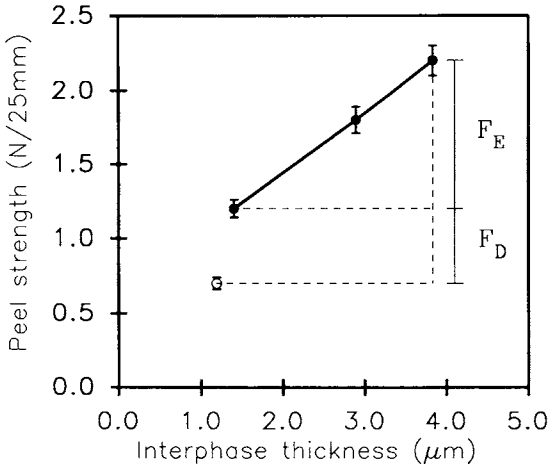

Figure 6 The effect of interphase thickness on peel strength of cellulose/PP laminates. Filled symbols represent treated fibers and empty ones represent untreated fibers. F_E and F_D are the contributions of entanglements and increased dispersive interactions, respectively, to the peel strength.

chain mobilities to form relatively strong entanglements. The alkenylsuccinic anhydride chain is too short to form entanglements, so the improvement in adhesion, as compared with untreated fibers, is probably caused by increased dispersion interactions. The plot in Figure 6, which indicates a proportionality between adhesion and interphase thickness, is a further illustration of the influence of diffusion on adhesion. The results allow an estimation of the contribution of entanglements, F_E, to the improvement of peel strength (as compared with untreated fibers). For example, when the compatibilizer of highest molecular weight is used, the contribution of entanglements is estimated to 70%, whereas increased dispersive interactions, F_D, would contribute with 30%.

CONCLUSIONS

The molecular weight of MAPP compatibilizer used for cellulose surface treatment was found to be crucial for the interfacial adhesion in cellulose–polypropylene composites. In all cases, the compatibilizing agents were immobilized on the cellulose fiber surface by chemical bonding. Graft density, surface free-energy data, and interaction measurements by IGC indicated the occurrence of significant stretching of compatibilizer chains away from the fiber surface, thus yielding brush-type interfaces. This behavior was thermodynamically favorable as

I. Graft densities of compatibilizer were relatively high.

II. The interfacial tension between the grafted chains and the matrix is low.

III. Stretching minimizes the presence of hydrophobic blocks in the high-energy regions of the hydrophilic cellulose surface.

A further indication of stretching and interdiffusion was the increase in interphase thickness with the increased molecular weight of the compatibilizer. This tendency was registered by evaluating yield stress data of composites according to the approach of Pukánszky. Adhesion measurements revealed a proportional relationship between interphase thickness and peel strength, indicating the considerable contribution of entanglements to the interfacial adhesion in these composite systems.

We thank Dr. Béla Pukánszky for valuable discussions. The Swedish National Board for Technical Development is gratefully acknowledged for financial support.

REFERENCES

1. C. Klason, J. Kubat, and P. Gatenholm, in *Viscoelasticity of Biomaterials,* ACS Symposium Series, W. Glasser, Ed., American Chemical Society, Washington, DC, 1990.
2. P. Zadorecki and A. J. Mitchell, *Polym. Compos.,* **10,** 2 (1989).
3. E. Galli, *Plast. Compound.,* **5**(3), 103 (1982).
4. R. G. Raj, B. V. Kokta, and C. Daneault, *J. Adhes. Sci. Technol.,* **3,** 55 (1989).
5. H. Dalväg, C. Klason, and H.-E. Strömvall, *Int. J. Polym. Mater.,* **11,** 9 (1985).
6. R. T. Woodhams, G. Thomas, and D. K. Rogers, *Polym. Eng. Sci.,* **24,** 1160 (1984).
7. M. J. Folkes, *Short Fibre Reinforced Thermoplastics,* Wiley, New York, 1982, pp. 24–27.
8. B. S. Hsiao and E. J. H. Chen, in *Controlled Interphases in Composite Materials,* H. Ishida, Ed., Elsevier, New York, 1990, pp. 613–622.
9. H. R. Brown, A. C. M. Yang, T. P. Russell, W. Volksen, and E. J. Kramer, *Polymer,* **29,** 1807 (1988).
10. S. Yukioka, K. Nagato, and T. Inoue, *Polymer,* **33,** 1171 (1992).
11. K. W. Allen, *J. Adhes.,* **21,** 261 (1987).
12. J. Comyn, in *Polymer Permeability,* J. Comyn, Ed., Elsevier, London, 1985, Chap. 5.
13. K. Cho, H. R. Brown, and D. C. Miller, *J. Polym. Sci. Part B Polym. Phys.,* **28,** 1699 (1990).
14. S. S. Voyutski, in *Autoadhesion and Adhesion of High Polymers,* Interscience, New York, 1963, Vol. 4.
15. A. G. Mikos and N. A. Peppas, *Polymer,* **30,** 84 (1989).
16. J. M. Felix and P. Gatenholm, *J. Appl. Polym. Sci.,* **42,** 609 (1991).
17. S. T. Milner, *Science,* **251,** 905 (1991).
18. B. Pukánszky, E. Fekete, and F. Tüdös, *Makromol. Chem. Macromol. Symp.,* **28,** 165 (1989).
19. L. I. Klushin and A. M. Skvortsov, *Macromolecules,* **24,** 1549 (1991).
20. S. Alexander, *J. Phys. (Paris),* **36,** 983 (1977).
21. P.-G. deGennes, *Macromolecules,* **13,** 1069 (1980).
22. S. T. Milner, T. A. Witten, and M. E. Cates, *Macromolecules,* **21,** 2610 (1988).
23. S. T. Milner, T. A. Witten, and M. E. Cates, *Macromolecules,* **22,** 853 (1989).
24. S. T. Milner, and T. A. Witten, *J. Phys. (Paris),* **49,** 1951 (1988).
25. C. M. Wijmans, J. M. H. M. Scheutjens, and E. B. Zhulina, *Macromolecules,* **25,** 2657 (1992).
26. R. C. Ball, J. F. Marko, S. T. Milner, and T. A. Witten, *Macromolecules,* **24,** 693 (1991).
27. G. H. Fredrickson, A. Ajdari, L. Leibler, and P. Carton, *Macromolecules,* **25,** 2882 (1992).
28. Reprint from *Pure Appl. Chem.,* **33**(2–3), 417 (1973).
29. B. S. Westerlind and J. C. Berg, *J. Appl. Polym. Sci.,* **36,** 523 (1988).
30. K. T. Hodgson, PhD dissertation, University of Washington, Seattle, 1986.
31. P. C. Painter, *Polymer,* **18,** 1169 (1977).
32. S. Wu, *J. Phys. Chem.,* **74,** 632 (1970).
33. S. Wu, *J. Adhes.,* **5,** 39 (1973).
34. B. Turcsányi, B. Pukánszky, and F. Tüdös, *J. Mater. Sci. Lett.,* **7,** 160 (1988).
35. B. Pukánszky, F. Tüdös, J. Jancar, and J. Kolarik, *J. Mater. Sci. Lett.,* **8,** 1040 (1989).
36. B. Pukánszky, *Composites,* **21,** 255 (1990).
37. B. Pukánszky, B. Turcsányi, and F. Tüdös, in *Interfaces in Polymer, Ceramic and Metal Matrix Composites,* H. Ishida, Ed., Elsevier, New York, 1988, p. 467.
38. B. Pukánszky, in *Structure and Properties of Polypropylene and Its Modified Systems,* J. Korger-Kocsis, Ed., Elsevier, London, to appear.
39. J. M. Felix and P. Gatenholm, in *Controlled Interphases in Composite Materials,* H. Ishida, Ed., Elsevier, New York, 1990, pp. 267–276.
40. H. Ishida, in *Proceedings of the 14th Annual Meeting of the Adhesion Society,* Clearwater, FL, Feb. 17–20, 1991.
41. K. L. Mittal, *Polym. Sci. Eng.,* **17,** 467 (1977).
42. S. Wu, *Polymer Interface and Adhesion,* Marcel Decker, New York, 1982.
43. M. E. Fowler, J. W. Barlow, and D. R. Paul, *Polymer,* **28,** 2145 (1987).
44. J. M. Felix, P. Gatenholm, and H. P. Schreiber, *Polym. Sci. Eng.,* to appear.

Received October 28, 1992
Accepted March 2, 1993